Proceedings Paper:
Zhou, M, Wang, X, Wu, Z et al. (2 more authors) (2020) Aneurysm Identification in Cerebral Models with Multiview Convolutional Neural Network. In: Crimi, A and Bakas, S, (eds.) Lecture Notes in Computer Science. BrainLes 2019, 17 Oct 2019, Shenzhen, China. Springer Nature , pp. 23-31. ISBN 9783030466398

https://doi.org/10.1007/978-3-030-46640-4_3

Aneurysm identification in cerebral models with multiview convolutional neural network

Mingsong Zhou[1], Xingce Wang[1⋆⋄], Zhongke Wu[1⋄], Jose M. Pozo[2], and Alejandro F. Frangi[2]

[1] Information Science and Technology College, Beijing Normal University, China
[2] Centre for Computational Imaging & Simulation Technologies in Biomedicine (CISTIB), School of Computing & School of Medicine, University of Leeds, Leeds, UK

Abstract. Stroke is the third most common cause of death and a major contributor to long-term disability worldwide. Severe stroke is most often caused by the rupture of a cerebral aneurysm, a weakened area in a blood vessel. The detection and quantification of cerebral aneurysms are essential for the prevention and treatment of aneurysmal rupture and cerebral infarction. Here, we propose a novel aneurysm detection method in a three-dimensional (3D) cerebrovascular model based on convolutional neural networks (CNNs). The multiview method is used to obtain a sequence of 2D images on the cerebral vessel branch model. The pretrained CNN is used with transfer learning to overcome the small training sample problem. The data augmentation strategy with rotation, mirroring and flipping helps improve the performance dramatically, particularly on our small datasets. The hyperparameter of the view number is determined in the task. We have applied the labeling task on 56 3D mesh models with aneurysms (positive) and 65 models without aneurysms (negative). The average accuracy of individual projected images is 87.86%, while that of the model is 93.4% with the best view number. The framework is highly effective with quick training efficiency that can be widely extended to detect other organ anomalies.

1 Introduction

Cerebral aneurysms are localized pathological dilatations of the cerebral arteries. Their rupture causes subarachnoid hemorrhage and is associated with a high morbidity and mortality rate [3]. For the average person, the incidence of aneurysms is $2-3\%$, and this proportion increases with age [13]. The early detection, growth monitoring and early treatment of aneurysms is the most effective sequence method for preventing aneurysmal rupture. However, the early detection of aneurysms in the brain vessel network is quite challenging.

Conventional aneurysm detection methods use the machine learning method to classify the aneurysm and vessel segments. Three main methods have been used to identify areas in which aneurysms may occur based on vascular shape, vascular skeleton, and image differences. Algorithms based on vascular morphology depend on the assumption that aneurysms are approximately spherical. Suniaga used Hessian

⋆ Corresponding author: wangxingce@bnu.edu.cn. Authors labeled with ⋄ have contributed equally to this work.

eigenvalues analysis to find spherical objects in 3D images [15]. Lauric constructed a geometric descriptor "writhe number" to distinguish between areas of tubular and nontubular structures [8]. The nontubular structures may be aneurysms. The dot filter [16] and blobness filter [15, 2, 4] have also been used to detect cluster structures in images based on prior knowledge of aneurysm morphology. The algorithm in [15, 16] is based on the skeleton to find the endpoints and branch points of the vascular structure and considers the distance between the endpoints and the branch points as the parameters of the classifier. Several hybrid algorithms have been used to train the classifier after feature extraction, incorporating classification strategies such as feature thresholding [8], rule-based systems [16] or case-based reasoning [6]. Almost all proposed algorithms are intended to work with magnetic resonance angiography (MRA) datasets; one, however, implements a multimodal approach on three-dimensional rotational angiography (3DRA) and computed tomography angiography (CTA) datasets [8]. The conventional methods for aneurysms detection are not generalizable; they extract features using descriptors of a dot filter or a blobness filter, or they extract customized features such as those related to geometry or distance. Since the use of CNNs has been successful in computer vision and image processing, many studies have examined aneurysm detection in medical images, such as MRA or 3DRA using a CNN. Jerman [5] used a Hessian-based filter to enhance spherical and elliptical structures such as aneurysms and attenuate other structures on the angiograms. Next, they boosted the classification performance using a 2D CNN trained on intravascular distance maps computed by casting rays from the preclassified voxels and detecting the first-hit edges of the vascular structures. Nakao [10] employed a voxel-based CNN classifier. The inputs of the network were 2D images generated from volumes of interest of the MRA images by applying a mixed-integer programming algorithm. The network architecture they used was not very deep: 4 convolution layers in one [5] and 2 convolution layers in the other [10]. More adjustable parameters (weights and bias) correspond to greater freedom of adjustment and a better approximation effect.

In medical image analysis, 2D images are widely used as input, but this approach is not well suited for aneurysm detection due to four limitations. First, we are interested in detecting aneurysms from different types of imaging modalities such as CT, MRA or 3DRA. The image resolution and file size may adversely affect the CNN performance. Second, even for the subjects having aneurysms, the percentage of the aneurysm volume data is quite small, which causes an imbalance of positive and negative samples in the learning process. Third, doctors detect aneurysms relying more on anisotropic shape representation than the intensity or texture in image, which results in a starting research point of separation aneurysms directly from the 3D cerebral mesh model. Finally, due to ethics and case selection problems, the availability of large population databases is not assured. Training on a small sample dataset is a common problem for many tasks in medical image analysis, such as segmentation or registration. To manage these limits, we detect aneurysms with a CNN in 3D cerebral mesh models with a pretrained neural network. After the segmentation and reconstruction of the cerebral vessel mesh model, the heterogeneous nature of the image format and resolution can be eliminated. The cerebral vessel network model can be divided into branch models with two or three bifurcations. Relative to the volume data of an image, the imbalance of the training sample of a model can be significantly

reduced. We overcome the influence of texture and intensity using the 3D cerebral branch model, which focuses on shape. In several view experiments, the classification accuracy of images is approximately 87%, while the classification accuracy of mesh models is approximately 92%. To our knowledge, we are the first group to apply CNN transfer learning to the aneurysm detection task on mesh models instead of medical images. The main contributions of the paper are as follows: (1)We present a novel aneurysm mesh model detection method based on a CNN. Due to the challenges of direct calculation convolution on the mesh model, we use the projection idea to change the 3D mesh model as a sequence of multiview projection images. (2)We use the transfer learning method and data augmentation of the input image to overcome the small training sample problem. The pretraining was performed using GoogleNet Inception V3 on ImageNet. We use the data augmentation with mirroring, rotation and flipping operations on the input image, which obtains 6 times more training samples than before.

2 Methodology

Problem formulation. The aneurysm detection task is formulated as a classification problem in this paper. Assume we have a training dataset composed of branches with or without aneurysms in a featured space $T = \{(b_1, l_1), (b_2, l_2), ..., (b_n, l_n)\} \subset B \times L$ where $B = \mathbb{R}^n$ is the feature vector space and $L = \{0, 1\}$ is the label space, where $l_i = 1$ represents that b_i includes an aneurysm (positive). The objective is to predict the label from the feature vector by a classification function. $\hat{l} = f(b)$ The training of $f(b)$ is based on minimization of the error between the predicted value $\hat{l_i}$ and the ground truth l_i, and the parameters in the classification function f are updated so that the classifier can be more effective.

Architecture of the network. The neural network of the project in called the multiview aneurysm model label network ($MVML$) with combined f^G and f^C. We consider as a classifier the pretrained GoogleNet Inception V3 (f^G) with a modified full-connection layer (f^C). The feature vector is each of the 2D images generated from multiview rendered images of the mesh models, which are used as inputs of the network. The outputs of the network are two probability values, corresponding to the negative and positive cases. Finally, the accuracy of the mesh model is determined by majority voting according to the image accuracy. Fig. 1 shows the framework of aneurysm detection proposed in this paper.

Case selection The positive dataset (vessel model with aneurysms) of 56 patients is drawn from a large multicenter database created within the EU-funded project @neurIST [9] based on the 3DRA image. The negative model set (vessel model without aneurysms), derived from the public dataset distributed by the MIDAS Data Server at Kitware Inc. [1], The segments of the mesh model included the similar branches as the positive dataset such as the anterior cerebral artery (ACA) or the internal carotid artery (ICA) bifurcation. No other information was considered during the selection process.

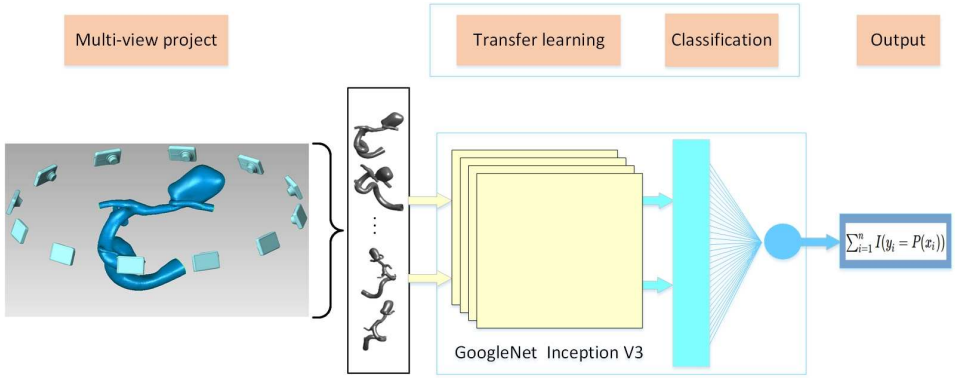

Fig. 1. Training process for the aneurysm detection with multiview CNN.

Multiview images from 3D aneurysm models . To obtain the multiview images from each 3D aneurysm model, the model coordination must be determined, and the projected method should be chosen. We first use PCA to determine the coordination of the mesh model. The vascular vertexes of each sample are denoted by $A = \{\left[x_i^j, y_i^j, z_i^j\right], j = 1, 2, 3 \ldots N\}, \mathrm{i} = 1, 2, 3 \ldots n_j$, where N denotes the number of samples within the dataset and n_j denotes the number of vascular vertexes in the dataset. The vertex coordinates of each sample are represented by $A_j(a) = \bar{A}_j + \sum_{i=1}^{n_j-1} a_i^j v_i^j$ $\bar{A}$ denotes the average vertex of the model j in the dataset and $a^j = [{a_1}^j, {a_2}^j, a_3^j, \ldots, a_{n_j-1}^j]$ denotes the eigenvalues of the covariance matrix in descending order of the model j and $v^j = [{v_1}^j, {v_2}^j, v_3^j, \ldots, v_{n-1}^j]$ denotes the corresponding orthogonal eigenvectors. The first three eigenvectors $[{v_1}^j, {v_2}^j, {v_3}^j]$, complemented with the right-hand rule, define the adapted coordinates of the 3D model j. The eigenvector corresponding to the largest eigenvalue is the rotation axis, while the one with the smallest eigenvalue of the first three is the beginning of the view projection. We then use the Phong reflection model [12] to create multiview images of the mesh model. We set up different numbers of viewpoints (virtual cameras) to obtain the mesh model rendering results. All the viewpoints (virtual cameras) are positioned on the ground plane and pointed toward the centroid of the mesh. We render the images from all the viewpoints to obtain a sequence of highly representative images of the mesh model. We shrink the white space around the view to enlarge its effective area. Different shading coefficients or illumination models do not affect our output descriptors due to the invariance of the learned filter to illumination changes as observed in an image-based CNN [7, 14]. Thus, the view color is set to gray. We create v rendered views by placing v virtual cameras around the mesh every $360/v$ degrees. The selection of the value for the hyperparameter v is discussed in detail in the experimental description. The Toolbox Graph [11] is used to generate the rendering result of the 3D mesh model.

Data augmentation with rotation and reflection. we enrich the dataset using mirroring, rotation, and flipping operations. Each image of the view is transformed to

create 2 additional images by flipping its horizontal and vertical edges, and another 3 additional images are created by rotating with 90, 180, and 270 degrees. Thus, we obtain 6 projected images from each view. The number of datasets is $v \times 6 \times 121$. With these treatments of the images, the difference of rotation axis orientation of the PCA eigenvector is eliminated.

Aneurysm labeling with transfer learning. To address the limitations of the aneurysm model dataset, we use the transfer learning method of the image to realize the learning result. The pretrained CNN based on large annotated image databases (ImageNet) is used for various classification tasks in the images of the different domains. The original network architecture can be maintained, and the network can be initialized with pretrained weights. The representation of each layer can be calculated from the representation of the previous layer. The end-to-end back-propagation algorithm, which combines feature extraction and classification processes, is widely used in CNN training. Generally, the convolution layers are considered as feature extractors, while the fully connected layers are seen as a classifier. The network architecture $MVML$ of the project is composed by f^G and f^C. We accept the pretrained GoogleNet Inception V3 model (f^G) as the feature extractors and the two-layer fully connected neuron network (f^C) as the classification. The latter outputs probabilities of the two classes with each input image view with the Softmax function. The cross-entropy loss function is adopted. $C = -\frac{1}{n}\sum_{i=1}^{n}[y_i \ln \hat{y}_i + (1 - y_i)\ln(1 - \hat{y}_i)]$ When the network training, only the weights of the fully connected neuron network are updated with the pretrained GoogleNet weights frozen. From the resulting decision for each view, we obtained the mesh group decision with majority voting,$E_i = \sum_{i=1}^{m} I(y_i = P(x_i)) \quad s.t. \quad I(y_i = P(x_i)) = \begin{cases} 1, & \text{if } y_i = P(x_i); \\ 0, & \text{if } y_i \neq P(x_i). \end{cases}$ where $m = k \times v$ is the total number of projected images per mesh model and v is the number of views. In our task, k is the multiplying factor of the data augmentation. x_i is the input image, and y_i is the label of the image. $P(x_i)$ is the prediction of the image by the classifier. The final label for the mesh model is the one satisfying $E_i > \frac{m}{2}$. For instance, for $v = 12$ and $k = 6$, an aneurysm mesh model with more than 36 different positive labeled projected images is assigned a final positive label. Model performance is measured by first classifying views of testing mesh models, and the classification results of all views through a majority voting process are used to obtain the final class label for each mesh model.

3 Experiments and Data Analysis

We conduct our research platform based on TensorFlow using an NVIDIA 960 M GPU on an Ubuntu 16.10 Linux OS 64-bit operating system. The initial fully connected classification is randomly set from 0 to 1. A stochastic gradient descent optimizer is employed to train the loss function of cross-entropy. A learning rate of 0.01 is suitable. The epoch step $K = 500$. The mini-batch size $N' = 128$. A five-fold cross-validation is used on the classifier performance. In the following, we test the effectiveness of the classification algorithm, the effect of the data augmentation, and the computational time of the network training.

Optimization of the view number hyperparameter First, we aim to verify the effect of the different view numbers v on the classification results using the accuracy of the mesh model and image data. We collect 3, 6, 9, 12, 15, and 18 views of the mesh model for the experiments. The views of the mesh models used for training the classifier are never used for testing. The overall prediction accuracy of the classifier on the image is evaluated, that is, the ratio of the number of images correctly classified to the total number of images evaluated (Table 1). The classification of each

Table 1. Classification accuracy of the image and mesh model(%).

View	3	6	9	12	15	18
Image	87.4±2.4	87.6 ±3.0	87.9 ±2.8	88.0 ±2.7	87.9 ±2.6	87.7 ± 2.8
Model	90.9 ±1.7	91.7±0.1	93.4 ± 2.0	92.6 ±1.6	92.6 ± 1.6	92.6 ± 1.6

view is only an instrumental task. The real result is the classification of the model. The mesh model label is achieved by a majority voting process based on the predicted probability for every view. The data show that when the number of views is large (such as 18), more images can be created to identify the aneurysms, but image mislabeling will greatly influence the results. For the proposed method, the equal possibility of aneurysms with the voting result of the images without aneurysms reduces the accuracy of the final result. The view number in this research is a nonlinear and unpredictable hyperparameter that greatly influences the result. The small view number of the model cannot offer sufficient images to reveal the aneurysm's shape; however, the large view number creates more branch clip images, resulting in mislabeling. From these results, we selected the number of views $v = 9$ as the optimal one, with a mean accuracy of 93.40%.

Effect of the data augmentation. To validate the effect of the data augmentation on the images, we test the model with or without data augmentation of the images. For the without-mirroring and rotation data augmentation view, the sizes of the dataset are 363, 726, 1089, 1452, 1815, and 2178. The accuracy of the classifier experiment on the images and the mesh model is shown in Table 2. Thus, the data augmentation appears not to greatly influence the accuracy. Inception V3 can bring out the strong features of the image to clearly illustrate aneurysms. However, the data augmentation has a strong influence on the mesh model. Without data augmentation, the accuracy of the model decreases by an average of 2%. First, the convolution

Table 2. Average classification accuracy of images and mesh models without data augmentation(%).

View	3	6	9	12	15	18
Image	87.9±3.3	87.9 ±3.7	88.3 ±3.4	88.6 ±2.7	87.9 ±2.5	87.7 ±2.9
Model	90.9 ±3.1	90.1±4.2	90.9 ± 4.1	91.8 ±2.5	90.9 ± 3.0	91.8 ± 3.6

layer of the Inception V3 is local on the image. After the data augmentation, the augmented image can be labeled identically to the original image. Second, the data augmentation brings more training data, which can increase the learning result of the classifier in the fully connected neural network. Third, deep learning with small training data is relatively instable in learning. More data can bring better results. In this case, the image data greatly influence the model accuracy.

Computation and Convergence Time. The time-consuming processes that are involved constitute a major challenge encountered in deep learning. We use transfer learning with GoogleNet to limit the training data and decrease the test time. The average change in the total lost function is smaller than 0.01 for 20 steps. We can identify the convergence of the training. The convergence steps of the training process are shown in Tables 3. For data that are not mirrored and rotated, the average numbers of convergence steps of the classifier in different views are approximately 330, 301, 327, 332, 331, and 300. The average numbers of convergence steps for different view classifiers are approximately 384, 361, 367, 348, 363, and 373 for different view classifiers through the mirroring and rotation data.

Table 3. Convergence steps of the training process.

view	3	6	9	12	15	18
without data augmentation	330	301	327	332	331	300
data augmentation	384	361	367	348	363	373

4 Conclusions

In this paper, we present a new multiview CNN to identify aneurysms in a 3D cerebrovascular model. No registration or alignment is necessary in the method for any of the models. With the projection of the 3D mesh model, we can obtain the multiview images. The transfer learning method with data augmentation is used in the model. The final mesh model identification is obtained by the voting algorithm. The method is simple to understand and implement. In a future study, we plan to incorporate postprocessing adjustment that is known to slightly improve the identification of some datasets. The development of a more sophisticated automatic adjustment will also necessitate further research.

Acknowledgement

The authors want to thank the anonymous reviewers for their constructive comments. This research was partially supported by the National Key Cooperation between the BRICS of China (No.2017YFE0100500), National Key R&D Program of China (No. 2017YFB1002604, No.2017YFB1402105) and Beijing Natural Science Foundation of China (No.4172033). AFF is supported by the Royal Academy of Engineering Chair in Emerging Technologies Scheme (CiET1819\19), and the OCEAN project (EP/M006328/1) and the MedIAN Network (EP/N026993/1) both funded by the Engineering and Physical Sciences Research Council (EPSRC).

References

1. Stephen R Aylward and Elizabeth Bullitt. Initialization, noise, singularities, and scale in height ridge traversal for tubular object centerline extraction. *IEEE Transactions on Medical Imaging*, 21(2):61–75, 2002.
2. Clemens M Hentschke, Oliver Beuing, Rosa Nickl, and Klaus D Tönnies. Detection of cerebral aneurysms in MRA, CTA and 3D-RA data sets. In *Proceedings of SPIE - The International Society for Optical Engineering*, page 83151I, 2012.
3. J. W Hop, G. J.E Rinkel, A. Algra, and van Gijn J. Case-fatality rates and functional outcome after subarachnoid hemorrhage: a systematic review. *Stroke*, 28(3):660–664, 1997.
4. Tim Jerman, Franjo Pernuš, Boštjan Likar, and Žiga Špiclin. Computer-aided detection and quantification of intracranial aneurysms. In *International Conference on Medical Image Computing and Computer Assisted Intervention*, pages 3–10, 2015.
5. Tim Jerman, Franjo Pernus, Boštjan Likar, and Žiga Špiclin. Aneurysm detection in 3D cerebral angiograms based on intra-vascular distance mapping and convolutional neural networks. In *IEEE International Symposium on Biomedical Imaging*, pages 612–615, 2017.
6. Syoji Kobashi, Katsuya Kondo, and Yutaka Hata. Computer-aided diagnosis of intracranial aneurysms in mra images with case-based reasoning. *IEICE transactions on information and systems*, 89(1):340–350, 2006.
7. Alex Krizhevsky, Ilya Sutskever, and Geoffrey E Hinton. Imagenet classification with deep convolutional neural networks. In *Advances in neural information processing systems*, pages 1097–1105, 2012.
8. Alexandra Lauric, Eric Miller, Sarah Frisken, and Adel M Malek. Automated detection of intracranial aneurysms based on parent vessel 3D analysis. *Medical image analysis*, 14(2):149–159, 2010.
9. Villa-Uriol MC1, Berti G, Hose DR, Marzo A, Chiarini A, Penrose J, Pozo J, Schmidt JG, Singh Pand Lycett R, Larrabide I, and Frangi AF. @neurist complex information processing toolchain for the integrated management of cerebral aneurysms. *Interface Focus*, 1(3):308–319, 2011.
10. Takahiro Nakao, Shouhei Hanaoka, Yukihiro Nomura, Issei Sato, Mitsutaka Nemoto, Soichiro Miki, Eriko Maeda, Takeharu Yoshikawa, Naoto Hayashi, and Osamu Abe. Deep neural network-based computer-assisted detection of cerebral aneurysms in MR angiography. *Journal of Magnetic Resonance Imaging*, 47(4):948–953, 2018.
11. Gabriel Peyre. *MATLAB central file exchange select*. 2 edition, 2009.
12. Bui Tuong Phong. Illumination for computer generated pictures. *Communications of the ACM*, 18(6):311–317, 1975.
13. Gabriel JE Rinkel, Mamuka Djibuti, Ale Algra, and J Van Gijn. Prevalence and risk of rupture of intracranial aneurysms: a systematic review. *Stroke*, 29(1):251–256, 1998.
14. Hang Su, Subhransu Maji, Evangelos Kalogerakis, and Erik Learned-Miller. Multi-view convolutional neural networks for 3D shape recognition. In *Computer Vision and Pattern Recognition*, pages 945–953, 2015.
15. Santiago Suniaga, Rene Werner, Andre Kemmling, Michael Groth, Jens Fiehler, and Nils Daniel Forkert. Computer-aided detection of aneurysms in 3D time-of-flight MRA datasets. In *International Workshop on Machine Learning in Medical Imaging*, pages 63–69, 2012.
16. Xiaojiang Yang, Daniel J Blezek, Lionel TE Cheng, William J Ryan, David F Kallmes, and Bradley J Erickson. Computer-aided detection of intracranial aneurysms in MR angiography. *Journal of digital imaging*, 24(1):86–95, 2011.